FEBS Letters 562 (2004) 22–26 FEBS 28155

A thermostable manganese-containing superoxide dismutase from pathogen *Chlamydia pneumoniae*

Jing Yu, Xiaomin Yu, Jianhua Liu*

College of Life Sciences and Technology, Shanghai Jiaotong University, 1954 Hua-shan Road, Shanghai 200030, PR China

Received 17 December 2003; revised 2 February 2004; accepted 2 February 2004

First published online 2 March 2004

Edited by Thomas L. James

Abstract The gene CP0718 encoding a putative manganese-containing superoxide dismutase of *Chlamydia pneumoniae* AR39 was cloned and expressed in *Escherichia coli*. Characterization showed that the expressed protein with a monomeric molecular mass of 23.1 kDa had superoxide dismutase (SOD) activity and the cofactor of CpSOD was a bivalent manganese cation. It is unexpected that this enzyme was hyperthermostable, and maintained about 90% activity after incubation at 70°C for 60 min. Manganese binding residues found in the SOD sequences from different species are conserved in CpSOD. Bioinformatics analysis compared with *Propionibacterium shermanii* MnSOD was performed to elucidate the CpSOD hyperthermostability based on amino acid sequences.

Key words: Superoxide dismutase; Expression; Purification; Thermostability; *Chlamydia pneumoniae*

1. Introduction

Superoxide dismutases (SODs) are vital metalloenzymes that constitute one of the major defense mechanisms of cells against oxidation stress by catalyzing transformation of superoxide anion into molecular oxygen and hydrogen peroxide in all oxygen-metabolizing organisms and in some anaerobes [1]. The catalytic mechanism involves sequential oxidation and reduction of the metal ion, and provides for electrostatic channeling of superoxide radicals to the active site. SODs are classified into four types with respect to their metal cofactor, (1) copper-zinc type (Cu/ZnSOD), (2) manganese type (MnSOD), (3) iron type (FeSOD) and (4) nickel type (Ni-SOD) [2,3].

MnSOD often exists in prokaryotes and in mitochondria of eukaryotes [4]. This protein was reported to suppress cancer cell growth [5,6] and contribute to the virulence of many human-pathogenic bacteria through its ability to neutralize toxic levels of reactive oxygen species generated by the host [7–9]. MnSOD was found to be effective as an anti-inflammatory agent and the half-life of MnSOD in serum was 5–6 h, while that of Cu/ZnSOD was only 6–10 min, indicating that MnSOD may be superior to Cu/ZnSOD for the treatment of chronic diseases [10].

Chlamydia pneumoniae, a pathogenic eubacterial parasite for humans, infects the mucosal surfaces of the respiratory tract causing pharyngitis, bronchitis and pneumonitis. Recent epidemiological data also suggest that *C. pneumoniae* may disseminate from the respiratory tract to produce vascular infection and contribute to atherogenesis [11]. The genome of *C. pneumoniae* AR39 has been completely sequenced [12]. Only a single gene, CP0718, has a high homology to MnSODs from other species. However, this prediction was not confirmed experimentally.

In this paper, we report the putative SOD of *C. pneumoniae* AR39 (CpSOD) expressed in *Escherichia coli* and characterized in vitro. Our experiments indicated that the cofactor of CpSOD was a bivalent manganese cation and the protein was thermostable. Bioinformatics analysis was used to interpret the requirement of manganese ion and hyperthermostability based on the CpSOD sequence.

2. Materials and methods

2.1. Materials

T4-DNA ligase, *Pyrobest*™ DNA polymerase and restriction endonucleases were obtained from TaKaRa (Dalian, China). pET expression system including expression vectors, *E. coli* strain BL21(DE3) pLysS, and nickel-nitrilotriacetic acid (Ni-NTA) His·Bind® Resin were purchased from Novagen (Madison, WI, USA). SOD assay kit was purchased from Nanjing Jiancheng Biotech (Nanjing, China). Oligodeoxyribonucleotides were synthesized by Sangon Biotech (Shanghai, China). *C. pneumoniae* AR39 genomic DNAs were kindly offered by Dr. Jin Huang at Dr. Stephen Lory's laboratory (Harvard Medical School, Cambridge, MA, USA). All other chemicals were of analytical grade.

2.2. Construction of the expression plasmid pET-CpSOD

Polymerase chain reaction (PCR) amplification was used to prepare CpSOD gene with *C. pneumoniae* AR39 genomic DNA as templates and oligodeoxynucleotides (upstream 5′-GGGGGCATATGAGTT-TTGTTCCTTATTC-3′ and downstream 5′-GGGGGAAGCTTATT-TAGATGATATTATTT-3′) as primers. In order to be cloned into plasmid pET-28a in correct translation frame, an *Nde*I site and a *Hin*dIII site were introduced in the upstream and the downstream primer, respectively. The PCR products were inserted into pET-28a digested with *Nde*I and *Hin*dIII. DNA sequencing was used to confirm the construct pET-CpSOD.

2.3. Expression and purification of CpSOD

The *E. coli* strain BL21(DE3) pLysS transformed with plasmid pET-CpSOD was induced with 0.5 mM isopropyl-1-thio-β-D-galactopyranoside (IPTG) for 3–5 h with the protocol offered by Novagen

*Corresponding author. Fax: (86)-21-5474 3192.
E-mail address: jianhualiudl@sjtu.edu.cn (J. Liu).

Abbreviations: CpSOD, superoxide dismutase of *Chlamydia pneumoniae* AR39; PsSOD, superoxide dismutase of *Propionibacterium shermanii*; MnSOD, manganese-containing superoxide dismutase; PCR, polymerase chain reaction; IPTG, isopropyl-1-thio-β-D-galactopyranoside; Ni-NTA, nickel-nitrilotriacetic acid

0014-5793/04/$30.00 © 2004 Published by Elsevier B.V. on behalf of the Federation of European Biochemical Societies.
doi:10.1016/S0014-5793(04)00170-X

company except that 800 μM $MnCl_2$ were also added when induction was initiated. Expressed proteins were purified by affinity chromatography on the Ni-NTA His·Bind® Resin (Novagen) column under denaturing conditions and renatured by dialyzing against 50 μM $MnCl_2$, 50 mM phosphate potassium (pH 7.8) with decreasing urea concentrations (from 4 M to 0 M) for 48 h at 4°C. Renatured CpSOD was then dialyzed extensively against 50 mM potassium phosphate buffer (pH 7.8) and stored at −20°C until further use. Protein concentration was determined by Bradford's method [13] based on a standard curve with bovine serum albumin. Sodium dodecyl sulfate–polyacrylamide gel electrophoresis (SDS–PAGE) was performed with Laemmli's Tris-glycine buffer system [14].

2.4. SOD activity assays

SOD activity was assayed with a SOD assay kit based on the cytochrome *c*–xanthine oxidase method [15]. One unit of activity was defined as the amount of enzyme which inhibits the rate of cytochrome *c* reduction by 50%. Different concentrations of $MnCl_2$ were added to the assay system in order to address the effects of $MnCl_2$ on the activities.

2.5. pH stability assay

CpSOD was incubated in 50 mM acetate buffer (pH < 6), phosphate buffer (pH 6–9), or borate buffer (pH > 9) containing 0 or 50 μM $MnCl_2$ at 30°C for 10 min, and then dialyzed against 50 mM potassium phosphate (pH 7.8). The remaining activities were determined.

2.6. Thermal stability assay

CpSOD was incubated in 50 mM potassium phosphate (pH 7.8) containing 0 or 50 μM $MnCl_2$ at different temperatures and the remaining activities were measured.

2.7. Structure analysis

Amino acid sequences and the crystal structure of *Propionibacterium shermanii* MnSOD were extracted from the protein entries in SwissProt and Protein Data Bank, respectively. Multiple sequence alignments were performed with ClustalW [16]. Secondary structures of CpSOD and PsSOD were generated using the InsightII molecular simulation software (2000 version). Solvent-accessible surface and buried surface areas were calculated with the Surface option in InsightII molecular simulation software.

3. Results and discussion

3.1. Construction of the expression plasmid pET-CpSOD

Expression plasmid pET-CpSOD was confirmed by DNA sequencing. In order to purify the recombinant proteins with Ni-NTA His·Bind® Resin affinity chromatography, the cloned CpSOD was fused with a 6×histidine tag at the N-terminus.

3.2. Expression and purification of CpSOD

CpSOD expression was induced with IPTG and Mn^{2+}. Prolonged induction and Mn^{2+} added simultaneously with IPTG would produce larger amounts of the recombinant CpSOD (data not shown). After recovery through Ni-NTA His·Bind® Resin chromatography under denaturing conditions, the expressed CpSODs were renatured. The specific activities of proteins obtained by affinity purification under native conditions were similar to those of proteins recovered by denaturing affinity purification followed by renaturing. In order to obtain larger amounts of expressed proteins, purification under denaturing condition followed by renaturing would be a better choice since CpSOD was expressed mainly as inclusion bodies (data not shown). Purified products were more than 95% pure as examined by 15% SDS–PAGE (Fig. 1). The specific activities of CpSOD were about 800 U/mg measured by SOD assay kit. The rough size of CpSOD subunit determined by SDS–PAGE was 23.1 kDa, coinciding with a mass value of 23 526.07 Da deduced from the CpSOD gene (Fig. 1).

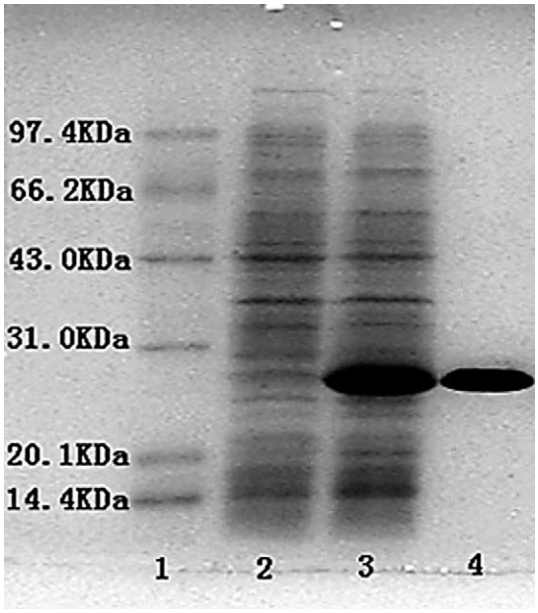

Fig. 1. SDS–PAGE analysis of CpSOD expressed in *E. coli* BL21(DE3) pLysS cell. 15% SDS–polyacrylamide gel was stained with Coomassie brilliant blue after electrophoresis. Lane 1, molecular weight markers; lane 2, total cell protein extracts before induction; lane 3, total cell protein extracts induced with IPTG and Mn^{2+} for 5 h; lane 4, purified CpSODs recovered by Ni-NTA chromatography.

3.3. Effects of Mn^{2+} on the enzymatic activities

Under the denaturation procedure, CpSOD was purified as apoprotein. Appropriate amounts of Mn^{2+} contained in the renaturing buffer were absolutely required for CpSOD renaturing (Table 1) [17]. No activity of CpSOD renatured without Mn^{2+} was detected under our assay condition, even when Mn^{2+} was supplied in the assay buffer. These observations demonstrated that Mn^{2+} was not only a cofactor for this enzyme, but also a key factor for correct protein folding. However, different concentrations of Mn^{2+} (from 0 to 50 μM) contained in the assay buffer contributed little to the enzymatic activities (Fig. 2).

3.4. pH stability assay

Activity profiles of CpSOD were investigated at 30°C be-

Table 1
Specific activities of CpSODs from different preparation conditions

	Native condition	Denaturing condition[a]			
Addition of Mn^{2+} (μM)	0	0	4	20	50
Specific activity (U/mg)	840	0	375	792	803

[a]Purified CpSODs were renatured under different Mn^{2+} concentrations and then dialyzed extensively against 50 mM potassium phosphate buffer (pH 7.8) containing no Mn^{2+}.

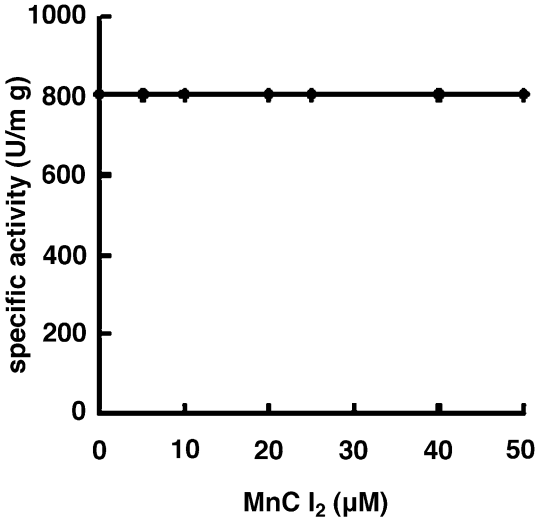

Fig. 2. Effects of $MnCl_2$ on CpSOD activities. CpSOD 1 μM was incubated in potassium phosphate (pH 7.8) containing 0 μM, 5 μM, 10 μM, 20 μM, 25 μM, 40 μM or 50 μM $MnCl_2$. The activities were determined by the cytochrome *c* test.

tween pH 2.5 and 11.5 (Fig. 3). With or without 50 μM $MnCl_2$, the purified proteins were stable between pH 6.0 and 8.0; the activity decreased a little in the regions of pH 8.0–9.0 and pH 4.0–6.0, but disappeared rapidly out of this range. This result is similar to that of the reported MnSODs of *Phanerochaete chrysosporium* [18] and *P. shermanii* [19]. It has been suggested that this inactivation might be triggered by the release of Mn^{2+} from the protein [19].

3.5. Thermostability and structure analysis

The thermostability was investigated by pre-incubating the enzyme in 50 mM potassium phosphate (pH 7.8) containing

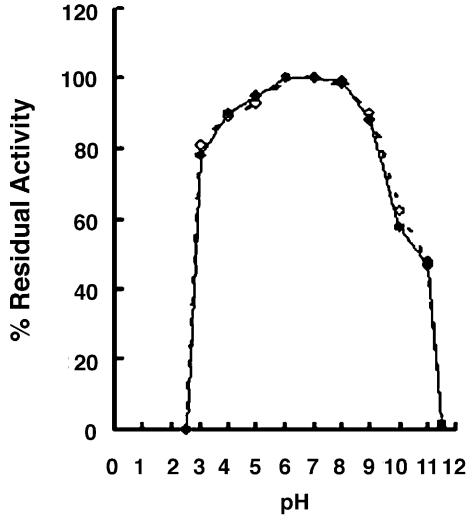

Fig. 3. pH stability of CpSOD. CpSOD 1 μM was incubated in 50 mM acetate, phosphate, or borate buffers containing 0 or 50 μM $MnCl_2$ with different pHs at 30°C for 10 min and then pH was restored to 7.8 by dialyzing against 50 mM potassium phosphate (pH 7.8). The remaining activities were determined by the cytochrome *c* test. The solid lines and symbols denote the buffer containing 0 μM $MnCl_2$, the dotted lines and symbols denote the buffer containing 50 μM $MnCl_2$.

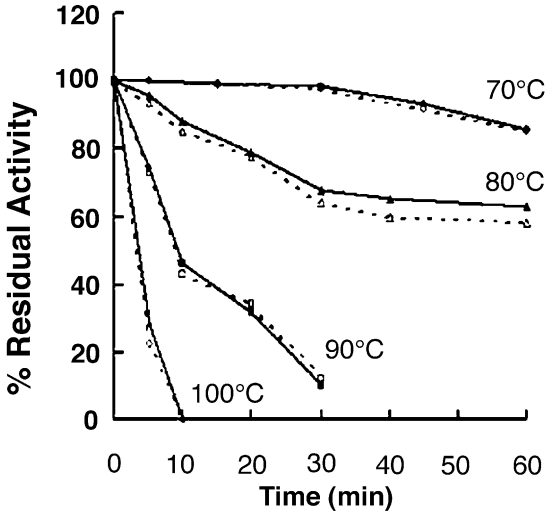

Fig. 4. Thermal stability of CpSOD. CpSOD 1 μM was incubated in 50 mM potassium phosphate (pH 7.8) containing 0 or 50 μM $MnCl_2$ at different temperatures. The remaining activities were determined by the cytochrome *c* test. (◇, ◆) 100°C; (□, ■) 90°C; (△, ▲) 80°C; (○, ●) 70°C. The solid lines and symbols denote the buffer containing 0 μM $MnCl_2$, the dotted lines and symbols denote the buffer containing 50 μM $MnCl_2$.

0 or 50 μM $MnCl_2$ at different temperatures. The activity was maintained at about 90% after incubation at 70°C for 60 min. Even after heating the enzyme at 95°C for 30 min, no apparent inactivation was observable (Fig. 4). These results indicate that CpSOD were thermostable, which was in contrast to MnSODs of *P. chrysosporium* [18] and *P. shermanii* [19], which were inactivated rapidly at 70°C.

The high thermal stability and broad pH stability of recovered CpSOD are also not affected by addition of $MnCl_2$ up to 50 μM in the assay buffer. This implies that Mn^{2+} added to the renaturing buffer only served as a cofactor to CpSOD, unlike other salts/molecules with positive and negative charges that are known to stabilize proteins in general by destabilizing the denatured form [19,20].

Comparing the amino acid sequence of CpSOD with those MnSODs whose high-resolution X-ray structures are available at present, Mn^{2+} binding residues are H30, H78, H170 and D166 (Fig. 5). Using InsightII software, the secondary structures for CpSOD and PsSOD were generated based on the Kabsch–Sander protein classification algorithm [21]. The overlapped secondary structures of CpSOD and PsSOD indicated that there are three obvious differences between the two structures (Fig. 6). (1) An excessive α-helix G, composed of residues 151–158, was present in CpSOD but absent in PsSOD. (2) α-helix C was present in CpSOD but absent in PsSOD and α-helices B and C are parallel in CpSOD. The hydrophobic interactions formed by the side chains of L41, L45, L48, L60, L63 and L67 increase the stability of CpSOD (Fig. 7). (3) The α-helix H in CpSOD was longer than that in PsSOD.

Besides the above helical variations, other factors would also contribute to the thermostability. We compared these factors including total solvent access areas, buried surface areas, numbers of charged residues and numbers of hydrophobic residues (Table 2). The numbers of hydrophobic residues and aromatic residues are similar in CpSOD and PsSOD,

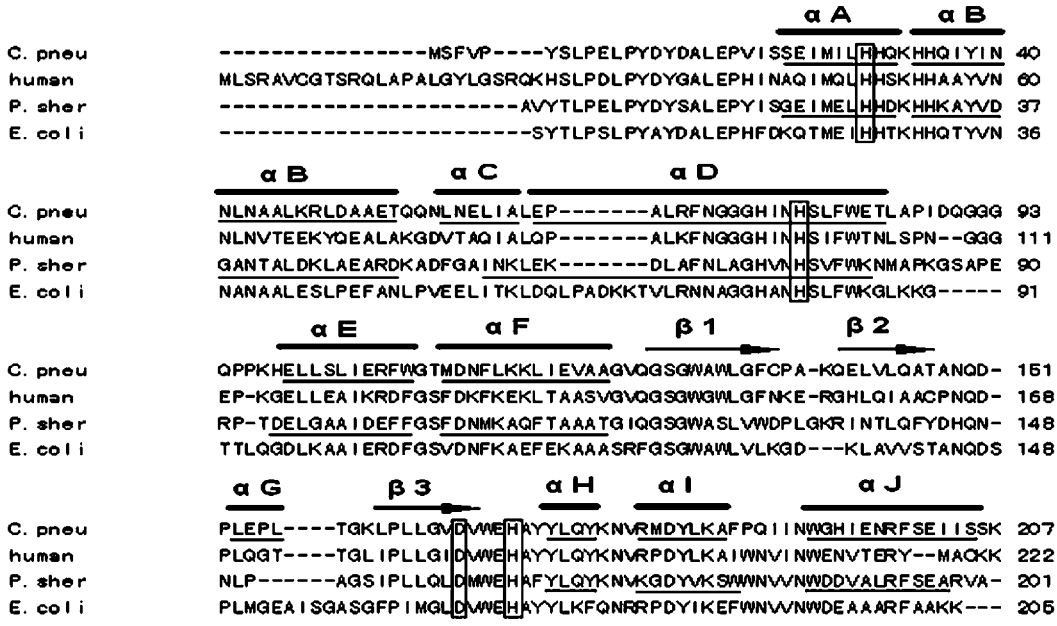

Fig. 5. Sequence alignment from various species. Amino acid sequences were aligned using the program ClustalW. Secondary structure elements were assigned with the InsightII molecular simulation software. Residues involved in the metal center are boxed with rectangles. Bold lines and arrows indicate residues involved in α-helices and β-sheets, respectively. Abbreviations: C. pneu, *C. pneumoniae*; P. sher, *P. shermanii*; E. coli, *E. coli*; human, human mitochondria.

but there are more L and I residues in CpSOD than in PsSOD. L and I residues have larger surface areas compared with other apolar and non-aromatic residues, leading to an increased buried surface area in CpSOD, which is the surface buried away from solvent when the protein folds. These increased buried surfaces strengthen the hydrophobic interactions. The increased hydrophobic interactions, additional helices, longer helix and paralleling helices B and C could contribute to the hyperthermostability of CpSOD.

Acknowledgements: We thank Dr. Jin Huang (Harvard Medical School, Cambridge, MA, USA) for graciously providing *C. pneumoniae* AR39 genomic DNA. This work was supported by the Natural Science Foundation of China (Grant 30170211).

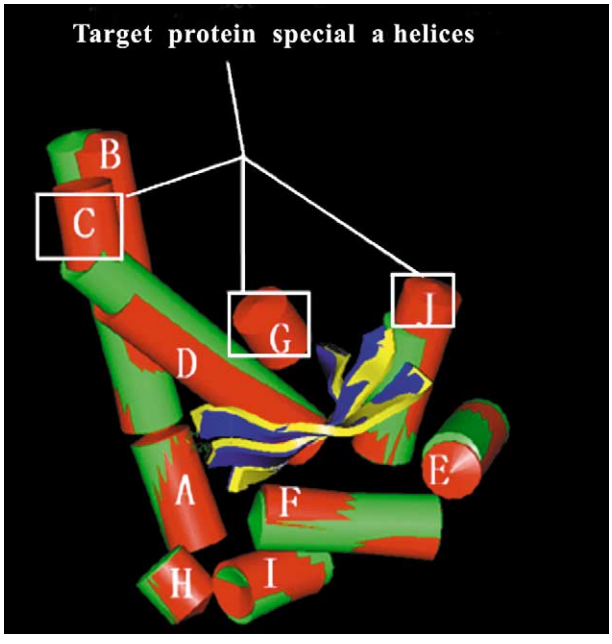

Fig. 6. The overlapped secondary structure of CpSOD and PsSOD generated based on the Kabsch–Sander protein classification algorithm by InsightII molecular simulation software. α-helices and β-sheets of CpSOD are in red and in blue, respectively; α-helices and β-sheets of PsSOD are in green and in yellow, respectively. (For interpretation of the references to color in this figure legend, the reader is referred to the web version of this article.)

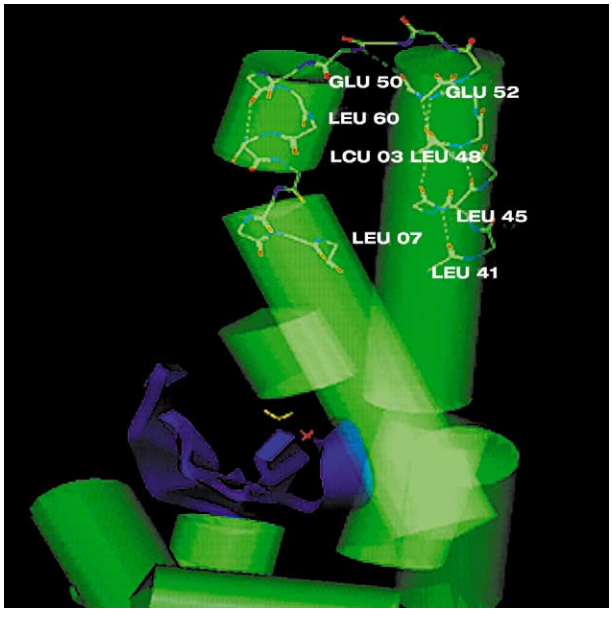

Fig. 7. The α-helix structure in CpSOD from residues 41–67 generated with InsightII molecular simulation software. α-helices are in green, β-sheets are in blue. (For interpretation of the references to color in this figure legend, the reader is referred to the web version of this article.)

Table 2
Structural properties of the compared CpSOD and PsSOD

	CpSOD	PsSOD
Number of amino acid residues	207	201
Number of charged residues (RKHDE)	47	53
Number of hydrophobic residues (AILFWV)	81	79
Number of aromatic residues	22	26
Number of L residues	28	19
Number of I residues	15	7
Total solvent access area (Å^2)	10 940.6	10 450.8
Buried surface area (Å^2)	23 022.0	22 722.7

References

[1] Fridovich, I. (1975) Annu. Rev. Biochem. 44, 147–159.
[2] Hassan, H.M. (1989) Adv. Genet. 26, 65–97.
[3] Youn, H.D., Kim, E.J., Roe, J.H., Hah, Y.C. and Kang, S.O. (1996) Biochem. J. 318, 889–896.
[4] Fridovich, I. (1986) Adv. Enzymol. Relat. Areas Mol. Biol. 58, 61–97.
[5] Bravard, A., Sabatier, L., Hoffschir, F., Ricoul, M., Luccioni, C. and Dutrillaux, B. (1992) Int. J. Cancer 51, 476–480.
[6] Cullen, J.J., Weydert, C., Hinkhouse, M.M., Ritchie, J., Domann, F.E., Spitz, D. and Oberley, L.W. (2003) Cancer Res. 63, 1297–1303.
[7] Yesilkaya, H., Kadioglu, A., Gingles, N., Alexander, J.E., Mitchell, T.J. and Andrew, P.W. (2000) Infect. Immun. 68, 2819–2826.
[8] Cox, G.M., Harrison, T.S., McDade, H.C., Taborda, C.P., Heinrich, G., Casadevall, A. and Perfect, J.R. (2003) Infect. Immun. 71, 173–180.
[9] Beaman, L. and Beaman, B.L. (1990) Infect. Immun. 58, 3122–3128.
[10] Gorecki, M., Beck, Y., Hartman, J.R., Fischer, M., Weiss, L., Tochner, Z., Slavin, S. and Nimrod, A. (1991) Free Radic. Res. Commun. 12–13, 401–410.
[11] Kuo, C.C., Grayston, J.T., Campbell, L.A., Goo, Y.A., Wissler, R.W. and Benditt, E.P. (1995) Proc. Natl. Acad. Sci. USA 92, 6911–6914.
[12] Read, T.D., Brunham, R.C., Shen, C., Gill, S.R., Heidelberg, J.F., White, O., Hickey, E.K., Peterson, J., Utterback, T., Berry, K., Bass, S., Linher, K., Weidman, J., Khouri, H., Craven, B., Bowman, C., Dodson, R., Gwinn, M., Nelson, W., DeBoy, R., Kolonay, J., McClarty, G., Salzberg, S.L., Eisen, J. and Fraser, C.M. (2000) Nucleic Acids Res. 28, 1397–1406.
[13] Bradford, M.M. (1976) Anal. Biochem. 72, 248–254.
[14] Laemmli, U.K. (1970) Nature 227, 680–685.
[15] McCord, J.M. and Fridovich, I. (1969) J. Biol. Chem. 244, 6049–6055.
[16] Thompson, J.D., Higgins, D.G. and Gibson, T.J. (1994) Nucleic Acids Res. 22, 4673–4680.
[17] Whittaker, M.M. and Whittaker, J.W. (2000) J. Biol. Inorg. Chem. 5, 402–408.
[18] Öztürk-Ürek, R., Bozkaya, L., Atav, E., Sağlam, N. and Tarhan, L. (1999) Enzyme Microb. Tech. 25, 392–399.
[19] Meier, B., Parak, F., Desideri, A. and Rotilio, G. (1997) FEBS Lett. 414, 122–124.
[20] Hess, D., Kruger, K., Knappik, A., Palm, P. and Hensel, R. (1995) Eur. J. Biochem. 233, 227–237.
[21] Kabsch, W. and Sander, C. (1984) Proc. Natl. Acad. Sci. USA 81, 1075–1078.